Study of e^+e^- and baryon-antibaryon production at PANDA (seeing from Gatchina)

S. I. Manaenkov

High Energy Physics Division Seminar

November 7, 2017, Gatchina, Russia

- $\bar{\text{P}}$ANDA Program
- The $\bar{\text{P}}$ANDA Experiment
- Electromagnetic Form Factors in Time-like Region
- Monte Carlo Simulation
- Competitiveness of the PANDA Experiment
- Hyperon-antihyperon production at PANDA
- Charmed Baryon-antibaryon production at PANDA
- Summary and Conclusions

$\bar{\mathrm{P}}$ANDA Program

- **Hadron spectroscopy**

  light mesons, baryons, charmonium,
  open charm,

  QCD exotics: glueballs, hybrids,
  X, Y, Z-states

- **Electromagnetic processes**

  time-like proton form factors,
  transition distribution amplitudes, TMDs

- **Hadronic interactions in nuclei**

  hyperons, hypernuclei,
  in medium-effects

PANDA Detector

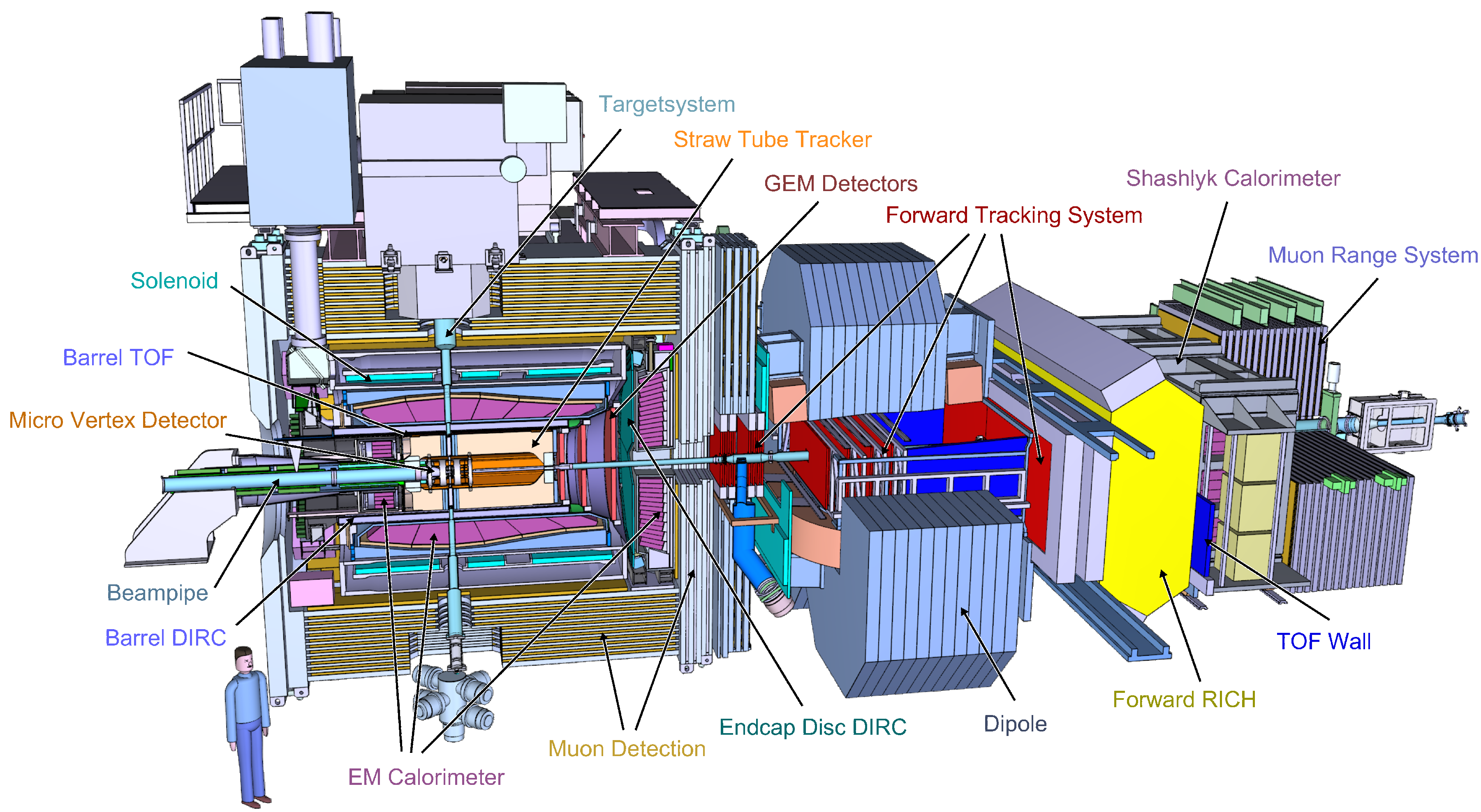

The $\bar{\rm P}$ANDA Experiment

- **Antiproton beam** $1.5 \le p \le 15$ **GeV/c,** $L = 2 \cdot 10^{32}$ **cm**$^{-2}$ **s**$^{-1}$
- **Targets: pellet, cluster-jet, liquid helium, polarized** ^{3}**He**

  Pellet Target: a steam of frozen hydrogen micro-spheres.
  Sizes 25 - 40 μ**m, the velocity of about 60 m/s,**
  lateral spread 1 mm, inter spacing 0.5 ÷ 5 mm.
  Plans: optical pellet tracking system (50 μ**m precision).**
  Cluster-jet Target: clusters of cold hydrogen gas with 10^3 **÷ 10**^{6}
  hydrogen molecules,
  homogeneous density with 10^{15} **atoms/cm**^{3}.
- **Magnets: central superconducting solenoid, forward dipole, correcting dipole magnets**

  Central solenoid: $R = 90$ **cm,** $l = 2.8$ **m,**
  magnetic field with $B = 2$ **T,** $\Delta B/B < 2\%$**.**
  Dipole magnet of forward spectrometer.
  Horizontal angles $|\theta_h| \le 10^\circ$**, vertical angles** $|\theta_v| \le 5^\circ$**.**
  $\delta p/p = 0.2\%$ **for** $p = 3$ **GeV/c, typical** $\delta p/p < 1.2\%$**.**

Electromagnetic Form Factor in Time-like Region

- **Kinematic variables**

  $P(p_1) + \bar{P}(p_2) \to e^-(k_1) + e^+(k_2)$,

  with $q^2 = s = (p_1 + p_2)^2 > 4m_p^2$, $\tau = \frac{q^2}{4m_p^2}$ **(**$\tau = 1$ **at the threshold).**

- **Sachs form factors**

  Form factors $G_E(s)$ **and** $G_M(s)$ **are complex for** $s \geq 4m_p^2$**.**
  Form factors are predicted in Quark Model, chiral perturbative theory, lattice calculations, perturbative QCD at $|q^2| \to \infty$.

- **Cross section for reaction $P\bar{P} \to e^-e^+$ in one-photon approximation**

$$\frac{d\sigma}{d\cos\theta_{cm}} = \frac{\pi\alpha^2(\hbar c)^2}{8m_p^2\sqrt{\tau(\tau-1)}}\left\{|G_M|^2(1+\cos^2\theta_{cm}) + \frac{|G_E|^2}{\tau}(1-\cos^2\theta_{cm})\right\}$$

$$\frac{d\sigma}{d\cos\theta_{cm}} = \sigma_0[1 + A\cos^2\theta_{cm}], \quad A = \frac{\tau - R^2}{\tau + R^2}, \quad R = |G_E/G_M|.$$

Electromagnetic Form Factor in Time-like Region

- **Total cross section**

$$\sigma_0 = \frac{\pi\alpha^2(\hbar c)^2}{8m_p^2\sqrt{\tau(\tau-1)}}|G_M^2|\left[1+\frac{R^2}{\tau}\right],$$

$$\sigma_{tot} = \frac{\pi\alpha^2(\hbar c)^2}{6m_p^2\sqrt{\tau(\tau-1)}}|G_M^2|\left[2+\frac{R^2}{\tau}\right].$$

- **Effective form factor**

$$|F_p|^2 = \frac{6m_p^2\sqrt{\tau(\tau-1)}}{\pi\alpha^2(\hbar c)^2(2+\frac{1}{\tau})}\,\sigma_{tot}$$

$$|F_p|^2 = |G_M|^2\,\frac{2+R^2/\tau}{2+1/\tau} \quad !!!$$

- **Form factor parameterization**

$$|G_{E,M}| = \frac{aG_D}{1+q^2/m_a^2}, \qquad G_D = (1+q^2/q_0^2)^{-2}.$$

World Data on Q^2-Dependence of Form Factor

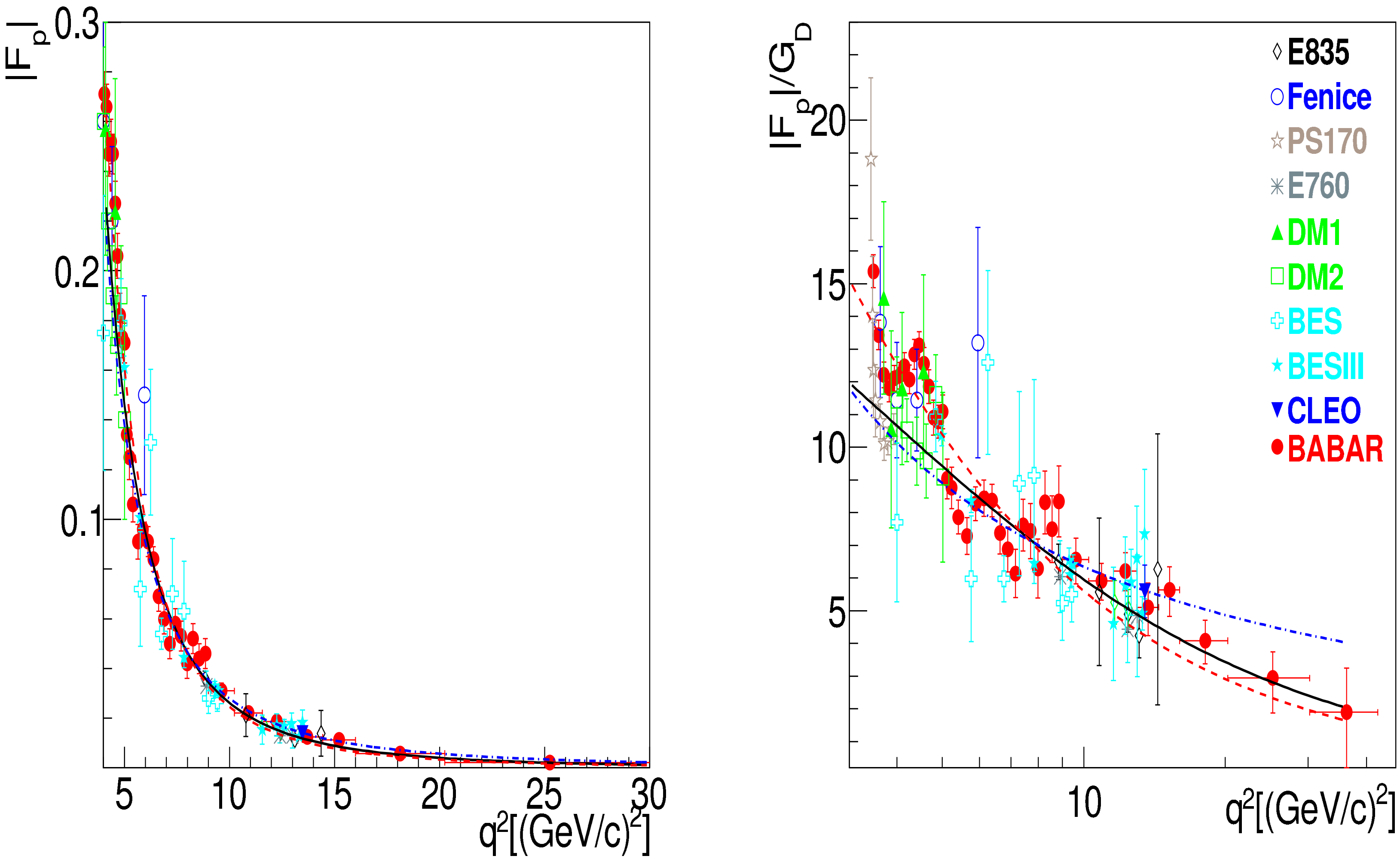

(a) (b)

Figure 2: q^2 dependence of the world data for $\bar{p}p \to e^+e^-$ and $e^+e^- \to \bar{p}p$. The effective proton TL FF, $|F_P|$, i extracted from the annihilation cross sections assuming $|G_E| = |G_M|$: E835 [35, 36], Fenice [37], PS170 [12], E760 [38] DM1 [39], DM2 [40, 41], BES [42], BESIII [14], CLEO [43], BABAR [32, 33]. Different parameterizations are show based on Eq. (11) (solid black and dashed red lines) and from Eq. (10) (dash-dotted blue line), as described in th text.

Electromagnetic Form Factors in Time-like Region

- **Asymptotic behaviour of form factors in space-like (SL) and time-like (TL) regions**

  $\lim_{q^2\to\infty}\left[\frac{F^{(TL)}(q^2)}{F^{(SL)}(-q^2)}\right] = 1,\ F \sim (1/q^2)^2$, **where** $F = G_E,\ \ G_M$**.**

  At $5 < q^2 < 10$ **GeV/c**^{2} $G_M^{(TL)}(q^2)/G_M^{(SL)}(-q^2) \sim 2 \div 3.$

  $G_M^{(TL)}(q^2)/G_M^{(SL)}(-q^2) \approx 1$ **at** $q^2 > 30$ **GeV/c**^{2}.

- **Two-photon exchange**

  Odd $\cos\theta_{cm}$ **terms appear due to interference of one-photon and two-photon exchanges which are zero at** $\theta_{cm} = 90°$.

  $$D = |G_M + \Delta G_M|^2(1+\cos^2\theta_{cm}) + \frac{|G_E+\Delta G_E|^2}{\tau}(1-\cos^2\theta_{cm})$$
  $$+2\sqrt{\tau(\tau-1)}\mathrm{Re}\left[\left(\frac{\mathrm{G_E}}{\tau} - \mathrm{G_M}\right)\mathrm{F_3^*}\right]\cos\theta_{\mathrm{cm}}(1-\cos^2\theta_{\mathrm{cm}}).$$
  $$\Delta G_{M,E}(q^2, -\cos\theta_{cm}) = -\Delta G_{M,E}(q^2, \cos\theta_{cm}),$$
  $$F_3(q^2, -\cos\theta_{cm}) = F_3(q^2, \cos\theta_{cm})$$

  F_3 **is measurable if** $|F_3/G_M| > 5\%$**.**

- **Background reactions**

1. $P + \bar{P} \to \pi^+ + \pi^-$, $\frac{\sigma(P+\bar{P}\to\pi^+ + \pi^-)}{\sigma(P+\bar{P}\to e^+ + e^-)} \sim (0.1 \div 0.35) \cdot 10^6$.

2. $P + \bar{P} \to \pi^0 + \pi^0$, $\frac{\sigma(P+\bar{P}\to 2\pi^0)}{\sigma(P+\bar{P}\to e^+ + e^-)} \sim 10^5$.

Dalitz channel: $\pi^0 \to e^- + e^+ + \gamma$,
$Br = \Gamma_{e^- e^+ \gamma} = (1.198 \pm 0.032)$%.

$\pi^0 \to 2\gamma$, $Br = (98.798 \pm 0.032)$%,

conversion $\gamma \to e^+ + e^-$ **in detector materials** ($\Gamma_{\gamma \to e^- e^+}$).

3. $P + \bar{P} \to \mu^+ + \mu^-$, $\frac{\sigma(P+\bar{P}\to\mu^+ + \mu^-)}{\sigma(P+\bar{P}\to e^+ + e^-)} \sim 1$,

weak decay before the iron wall:

$\mu^- \to e^- + \nu_\mu + \bar{\nu}_e$, **hence** $\mu^+ + \mu^- \to e^+ + e^- + X$,

$X =$ **neutrinos and antineutrinos.**

Monte Carlo Simulation at $q^2 = $ 5.40, 8.21, and 13.9 (GeV/c)^2

- **PANDA Detector Property**

  Beam $\frac{\Delta p}{p} \sim 10^{-5}$ (low intensity); $\frac{\Delta p}{p} \sim 10^{-4}$ (high intensity).

  Charged particle momentum resolution $\delta p/p \sim 10^{-2}$.

- **Background suppression factors**

  1. Background from $P + \bar{P} \to e^- + e^+ + X$.

     Even for $X = \pi^0$ background suppression factor $R_X > 10^8$ due to kinematical cuts.

  2. Background from $P + \bar{P} \to \pi^- + \pi^+$.

     Background suppression factor $R_{bg} > 10^8$ due to particle identification requirements only.

     If kinematical cuts are added the total suppression factor $R_{bg} > 10^{10}$, hence $\frac{N(P+\bar{P}\to e^-+e^+)}{N(P+\bar{P}\to \pi^-+\pi^+)} > 100$.

Monte Carlo Simulation at $q^2 =$ 5.40, 8.21, and 13.9 (GeV/c)^2

3. Background from $P + \bar{P} \to \pi^0 + \pi^0$.

a) Double Dalitz channel contains the factor $[\Gamma_{e^- e^+ \gamma}]^2 \sim 10^{-4}$. Rejection factor due to kinematical cuts $R_{kin} > 10^4$. The total background suppression factor $R_{bg} > 10^8$.

b) Dalitz channel for one π^0 and for another neutral pion $\pi^0 \to 2\gamma$, $\gamma \to e^- + e^+$ is proportional to $[\Gamma_{e^- e^+ \gamma}][\Gamma_{\gamma \to e^- e^+}]$. The process $\gamma \to e^- + e^+$ was not simulated with the real detector materials, but $\Gamma_{\gamma \to e^- e^+} \sim 1\%$. The total $R_{bg} > 10^8$.

c) $\pi^0 \to 2\gamma$, every γ quantum creates $e^- e^+$. The total suppression factor $R_{bg} > 10^8$.

4. Background from $P + \bar{P} \to \mu^+ + \mu^-$. Reaction was not simulated but this background is nor crucial since its cross section is close to $\sigma(P + \bar{P} \to e^- + e^+)$.

- **Signal-to-Background ratio for reaction $P + \bar{P} \to e^+ + e^-$ can be made about 100.**

Competitiveness of the PANDA Experiment

- Feasibility studies of time-like proton electromagnetic form factors at PANDA at FAIR, Eur. Phys. J. A52 (2016) 325.
  ...,S. Belostotski, G. Gavrilov, A. Izotov, S. Manaenkov, O. Miklukho, D. Veretennikov, A. Zhdanov, ...
- Comparison of the PANDA experiment with BES and Belle
  BESIII will measure $|G_E|$ and $|G_M|$ separately for the first time for $4.0 < q^2 < 9.5$ GeV/c^2 with statistical precision between 9% and 35%.
  Individual form factors will be measured by PANDA at $5.4 < q^2 < 13.9$ GeV/c^2 with fractional uncertainty between 2% and 48%.
  Belle and Belle II are working at KEKB from 1999 using Initial State Radiation (ISR) technique, but so far no estimation for form factors (FFs) has been presented. One disadvantage of ISR method is extraction of FFs in wide bins of q^2.
  In contrast, PANDA has high precision of q^2 measurement.

Hyperon-antihyperon Production at PANDA

- **Excited Strange Baryons**
  Data quality for excited states of Σ ($S = -1$) is poor.
  Data on excited states of Ξ ($S = -2$) and Ω ($S = -3$) is particularly scarce.
- **$\Xi\bar{\Xi}$-pair production**
  If for excited Ξ the production cross section is $\sim \sigma_{\Xi} = 2$ μb, then all decay channels $\Xi\pi$, $\Xi\pi\pi$, $\Lambda\bar{K}$, $\Sigma\bar{K}$, $\Xi\eta$ can be studied.
- **$\Omega\bar{\Omega}$-pair production**
  $\sigma_{\Omega\bar{\Omega}}$ was not measured. Theoretical estimate $\sigma_{\Omega\bar{\Omega}} = 2$ nb.
  For $L = 10^{32}$ cm^{-2} s^{-1} 700 $\Omega\bar{\Omega}$-pairs per hour.
- **Polarization phenomena**
  Measurements of the hyperon polarization versus s.
  Search for CP-violation: $A = \frac{\alpha\Gamma + \bar{\alpha}\bar{\Gamma}}{\alpha\Gamma - \bar{\alpha}\bar{\Gamma}}$, $D = \frac{\Gamma - \bar{\Gamma}}{\Gamma + \bar{\Gamma}}$;
  α is analyzing power, Γ is decay width.
  Standard Model: $A \sim 10^{-5}$, models beyond SM $A \sim 10^{-4}$.

Baryon-antibaryon Production at PANDA

Hyperon	Quarks	Mass MeV/c^2	$c\tau$ cm	Main Decay	Br %	α_Y
Λ	uds	1116	8.0	$p\pi^-$	64	+0.64
Σ^+	uus	1189	2.4	$p\pi^0$	52	-0.98
Σ^0	uds	1193	2.2$\cdot 10^{-9}$	$\Lambda\gamma$	100	–
Σ^-	dds	1197	2.4	$n\pi^-$	100	-0.07
Ξ^0	uss	1315	8.7	$\Lambda\pi^0$	99	-0.41
Ξ^-	dss	1321	4.9	$\Lambda\pi^-$	100	-0.46
Ω^-	sss	1672	2.5	ΛK^-	68	-0.03
Λ_c^+	udc	2286	6.0 $\cdot 10^{-3}$	$\Lambda\pi^+$	1	-0.91(15)
Σ_c^{++}	uuc	2454	—	$\Lambda_c^+\pi^+$	100	—
Σ_c^+	udc	2453	—	$\Lambda_c^+\pi^0$	100	—
Σ_c^0	ddc	2454	—	$\Lambda_c^+\pi^-$	100	—
Ξ_c^+	usc	2468	1.2 $\cdot 10^{-2}$	$\Xi^-\pi^+\pi^+$	seen	—
Ξ_c^0	dsc	2471	2.9 $\cdot 10^{-3}$	$\Xi^-\pi^+$	seen	-0.6(4)
Ω_c^0	ssc	2697	1.9 $\cdot 10^{-3}$	$\Omega^-\pi^+$	seen	—

$$W(\theta_B) = \frac{1}{4\pi}(1 - \alpha_Y P_Y \cos\theta_B); \qquad W_{\Sigma^0}(\theta_P) = \frac{1}{4\pi}(1 - \frac{1}{3}\alpha_\Lambda P_{\Sigma^0} \cos\theta_P).$$

Summary and Conclusions

- **The PANDA experiment will have a very small spread of the antiproton beam, high momentum and angular resolution in all 4π angular acceptance, and very efficient particle identification system.**
- **In the PANDA experiment, it will be possible to suppress by a factor $\sim 10^8$ the background processes. This permits to measure separately the electric and magnetic form factors of the proton in reaction $P + \bar{P} \rightarrow e^- + e^+$ with fractional precision of about a few per cents at $5.4 < q^2 < 13.9$ (GeV/c)^2.**
- **Two-photon exchange can be observed if its fractional contribution is greater than 5%.**
- **Production and decay of a great variety of hyperons and charmed baryons can be studied with high precision.**
- **The achieved statistics in the hyperon production will permit in principle to measure CP-violation effects of the order of 10^{-4}.**